Applied Microbiology and Biotechnology
https://doi.org/10.1007/s00253-018-9167-2

BIOTECHNOLOGICALLY RELEVANT ENZYMES AND PROTEINS

Bispecific affibody molecule targeting HPV16 and HPV18E7 oncoproteins for enhanced molecular imaging of cervical cancer

Shanli Zhu[1] · Jinshun Zhu[1] · Yiling Song[1] · Jun Chen[1] · Lude Wang[1] · Meng Zhou[1] · Pengfei Jiang[1] · Wenshu Li[1] · Xiangyang Xue[1] · Kong-Nan Zhao[1] · Lifang Zhang[1]

Received: 22 March 2018 / Revised: 4 June 2018 / Accepted: 9 June 2018

Abstract

High-risk human papillomavirus (HPV16 and HPV18) are now widely recognized as responsible for cervical cancer, which remains to be the most common gynecologic malignancy in women worldwide. It is well known that viral oncoproteins E6/E7 play key roles in HPV-associated cervical carcinogenesis. Thus, in vivo detection of the two oncoproteins may provide important diagnostic information influencing patient management. More recently, affibody molecules have been demonstrated to be a promising candidate for development as molecular imaging probes. Based on the two monomeric affibody molecules ($Z_{HPV16E7}$ and $Z_{HPV18E7}$) generated in our laboratory, here, we used a peptide linker $(Gly_4Ser)_3$ to link $Z_{HPV16E7}$ and $Z_{HPV18E7}$ to develop a novel heterodimeric affibody $Z_{HPV16E7}$–$(Gly_4Ser)_3$–$Z_{HPV18E7}$. Both biosensor and immunofluorescence assays have proved that the heterodimeric affibody molecule targeted simultaneously HPV16 and HPV18E7 proteins by binding to the viral oncoproteins. In vivo tumor-imaging experiments using the Dylight755-labeled heterodimeric affibody revealed that strongly high-contrast tumor retention of the heterodimers occurred in both HPV16- and HPV18-derived tumors of nude mice 0.5 h post-injection. The accumulation of Dylight755-labeled heterodimers in tumors was achieved over 48 h. Therefore, we believe that this novel heterodimeric affibody molecule has great potential utility in molecular imaging in vivo and diagnosis of HPV-associated cervical cancers.

Keywords Affibody molecule · Cervical cancer · Human papillomavirus · E7 · Oncoproteins

Introduction

Use of bi- or multispecific affinity proteins targeting simultaneously several disease-related proteins is emerging as novel strategy for accurate molecular diagnosis of diseases and reducing likelihood of drug resistance in cancer therapy (Kontermann 2012; Byrne et al. 2013). Several studies have shown that persistent infection of the cervix with high-risk HPV genotypes is necessary for its immediate precursor lesion, cervical intraepithelial neoplasia grade 3 (CIN3), and development of cervical cancer (Saslow et al. 2012). Epidemiological studies have shown that high-risk HPV is present in nearly 99% of cervical cancer cases (Walboomers et al. 1999). HPV16 is by far the most dominant carcinogenic genotype, responsible for 55–60% of the cervical cancer in the world, followed by HPV18 present in at least 15% of invasive cervical cancers (Walboomers et al. 1999; de Sanjose et al. 2010; Muñoz et al. 2003). Therefore, HPV-based cervical cancer screening is very important for predicting the incidences of invasive cancer. Published data have demonstrated improved efficacy and great protection of HPV-based compared with the cytology-based screening against invasive cervical cancers (Ronco et al. 2014; Ogilvie et al. 2017). Accurate diagnosis of cervical cancer, especially tumor's invasion and metastasis, is central to determine the appropriate treatment approach and measure the clinical outcome. As we

Shanli Zhu, Jinshun Zhu and Yiling Song contributed equally to this work.

Electronic supplementary material The online version of this article (https://doi.org/10.1007/s00253-018-9167-2) contains supplementary material, which is available to authorized users.

✉ Kong-Nan Zhao
knzhao888@hotmail.com

✉ Lifang Zhang
wenzhouzlf@126.com

[1] Institute of Molecular Virology and Immunology, Department of Microbiology and Immunology, School of Basic Medical Sciences, Wenzhou Medical University, Wenzhou 325035, Zhejiang, People's Republic of China

Published online: 25 June 2018

know, the standard surgical treatment for cervical cancer patients is radical hysterectomy with pelvic lymphadenectomy. However, up to now, no effective method can be used for intraoperative detection of lymph node metastasis, parametrical involvement, and deep cervical stromal invasion of cervical cancers.

HPV viral DNA fragments are frequently found to integrate into the host genome (Badaracco et al. 2002; Hopman et al. 2004; Romanczuk and Howley 1992). The integrated HPV DNA fragments include E6/E7 oncogenes and other viral DNAs. The integrated E6/E7 oncogenes express sustainably viral oncoproteins, which play the key roles in cervical carcinogenesis (Badaracco et al. 2002; Hopman et al. 2004; Romanczuk and Howley 1992). E6 and E7 protein impedes and degrades the normal physiological function of tumor suppressor p53 and pRb, respectively, which leads to transformation of human cells and thus contributing to cervical carcinogenesis (Scheffner et al. 1990; Roman and Munger 2013; Mirabello et al. 2017). It is well documented that E6 and E7 oncogenes are persistently retained and highly expressed in HPV-positive cervical cancer cells (Schwarz et al. 1985). Therefore, HPV E6/E7 oncoproteins act as appropriate targets for diagnostic and therapeutic strategies against HPV-associated tumors due to their specific expression in HPV infected tissues.

Affibody molecules are a class of small (58 amino acids, ~ 6 kDa), non-immunoglobulin affinity proteins based on the Z domain derived from staphylococcal protein A (Löfblom et al. 2010). Rapid tumor localization, fast clearance from blood, and non-specific compartments make them very attractive for many medical applications, including in vivo molecular imaging, receptor signal blocking, and delivery of toxic payloads (Frejd and Kim 2017; Ståhl et al. 2017). To date, over 400 studies published show that affibody molecules have been selected for targeting more than 40 different proteins and used as affinity moieties in a variety of applications (Ståhl et al. 2017). The affibody-targeted proteins include human epidermal growth factor receptor 2 (HER2), epidermal growth factor receptor (EGFR), human epidermal growth factor receptor 3 (HER3), vascular endothelial growth factor (VEGF), and HPV16E7 (Orlova et al. 2006; Andersson et al. 2016; Kronqvist et al. 2011; Fedorova et al. 2011; Xue et al. 2016). Furthermore, because of their small size, disulfide-independent and rapid-folding, affibody molecules are suitable for ideal candidates for developing bi- or multispecific affibody proteins. The size of multispecific affibody molecules remains to be small, for example, the molecular weight of multispecific affibody molecules that contain two or three binding domains was similar to a single-chain fragment variable (scFv) (Malm et al. 2014; Ekerljung et al. 2012; Friedman et al. 2009). Importantly, biosensor assays and cell-binding assays have shown that bispecific affibody molecules, targeting HER2 and HER3, EGFR, and HER2, can bind simultaneously to both proteins.

Currently, there is intense interest in developing bispecific affibody molecules targeting HPV16E7 and HPV18E7 oncoproteins that are highly associated with cervical cancer. In our previous studies, we engineered separately several affibody molecules from phage display library for specific binding of HPV16E7 (Xue et al. 2016) and HPV18E7 oncoprotein (Electronic supplementary material). The specific binding of the generated affibody molecules to HPV16E7 oncoprotein have been confirmed by in vitro biosensor assays and in vivo xenograft mouse model (Xue et al. 2016). Here, we report a novel format of the bispecific affibody molecules that bind simultaneously to the two oncoproteins. We describe characterization of bispecific heterodimeric HPV16 E7- and HPV18 E7-binding affibody molecules and their applications to molecular imaging in vivo in xenograft mice.

Material and methods

Production of bispecific affibody molecules

The gene fragments encoding $Z_{HPV16E7}$ (GenBank accession no. MH166809) and $Z_{HPV18E7}$ (GenBank accession no. MH166810, $Z_{HPV18E7:228}$, Figs. S1 and S2) were isolated by PCR amplification from recombinant plasmids pET21a(+)/$Z_{HPV16E7}$ and pET21a(+)/$Z_{HPV18E7}$ with high-fidelity DNA polymerase KOD plus neo (Toyobo Life Science, Japan). The dimeric constructs were generated by ligation of both DNA fragments into the prokaryotic expression vector pET21a(+) using T4 DNA ligase in subsequent cloning steps. Two domains were separated by 20-amino-acid-long $(Gly_4Ser)_3$ linker. In addition, homodimeric $Z_{HPV16E7}$–$Z_{HPV16E7}$ and $Z_{HPV18E7}$–$Z_{HPV18E7}$ and monomeric $Z_{HPV16E7}$ and $Z_{HPV18E7}$ were constructed as controls. DNA sequence of the bispecific affibody molecules was verified by DNA sequencing.

The His-tagged affibody variants were expressed in Escherichia coli *(E.coli)* BL21(DE3) cells and induced by addition of 1 mM isopropyl-L-thio-β-D-galactopyranoside (IPTG, Sigma-Aldrich Co., St. Louis, MO). After 4–6 h, the cultured cells were harvested and resuspended in PBS (pH 8.0). Then, the cells were disrupted by sonication on ice until the cells were thoroughly homogenized. After centrifugation at 12,000 rpm for 30 min at 4 °C, the supernatant was filtered with 0.45 μm filter and the proteins were loaded on an Ni-NTA agarose resin (Qiagen, Hilden, Germany) column and washed with PBS (pH 8.0), followed by washing buffer (20 mM sodium phosphate, 0.5 M NaCl, 10 mM imidazole, pH 8.0). The bound proteins were eluted with elution buffer (20 mM sodium phosphate, 0.5 M NaCl, 100 mM imidazole, pH 8.0). The purity and the correct molecular mass of the fusion proteins were confirmed by SDS-PAGE and Western

blot with the mouse anti-His monoclonal antibody (mAb) (MultiSciences Biothech Co., Ltd., China). Subsequently, the purified proteins were further dialyzed against PBS using Slide-A-Lyzer (Pierce, Rockford, IL, USA) according to the manufacturer's protocols. After determining concentration using bicinchoninic acid (BCA) protein quantitation method, the purified proteins were stored at − 80 °C.

Template-based structure prediction

Three-dimensional (3D) structure of the fusion proteins was predicted using SWISS-MODEL workspace, and the biophysical properties were calculated by submitting the amino acid sequence of bispecific affibody molecules on ExPASy server (https://swissmodel.expasy.org/interactive).

Biosensor interaction analysis

To assess the target binding of the bispecific affinity protein to HPV16E7 and HPV18E7, surface plasmon resonance (SPR) was performed on a Biacore T200 (GE Healthcare, Uppsala, Sweden). The HPV16E7 and HPV18E7 proteins served respectively as the ligands and were immobilized onto the surface of Sensor Chip CM5 (GE Healthcare), as described previously (Xue et al. 2016). Subsequently, eight different concentrations of each sample were prepared and injected over the chip surface to record sample binding to the surface. All SPR experiments were carried out with a flow rate of 30 μL/min at 25 °C. SPR data of the homodimeric molecules were fit with bivalent model and the others were fit globally using a 1:1 L binding model and analyzed by BIA evaluation 3.0.2 software.

Cell culture

Two cervical cancer cell lines and one melanoma cell line were obtained from the American Type Culture Collection (ATCC). SiHa cell (ATCC: HTB-35) expressing the HPV16 E7 protein, HeLa (ATCC: CCL-2) expressing HPV18E7 protein, and melanoma cell line A375 (ATCC: CRL-1619) negative for HPV DNA. All cell lines were maintained by serial passage in 5% CO_2 incubator at 37 °C and cultured in DMEM supplemented with 10% fetal bovine serum, 100 units/mL of penicillin, and 0.1 mg/mL of streptomycin.

Immunofluorescence detection

To determine whether the bispecific affibody molecule could simultaneously bind to the HPV16E7 and HPV18E7 native proteins, indirect immunofluorescence analysis was performed as previously described with minor modifications (Xue et al. 2016). Briefly, SiHa cell (expressing HPV16 E7 protein), HeLa cell (expressing HPV18 E7 protein), and A375 melanoma cell (negative for HPV DNA) were seeded on 24-well plates in 5% CO_2 incubator at 37 °C. Twenty-four hours later, the medium was replaced with fresh media supplemented with 100 μg/mL affibody molecules or wild Z_{WT} control. After incubation for 6 h, cells were washed with PBS and fixed with 4% paraformaldehyde (PFA) at room temperature (RT) for 10 min. Subsequently, treated cells were permeabilized by 0.3% Triton X-100 at RT for 10 min, followed by blocking with 20% FBS in RPMI-1640. Two hours later, the cells were used for analyzing of bispecific affibody molecules binding to HPVE7 proteins by mouse anti-His mAb, followed by the addition of secondary antibodies at RT for 1 h. The nuclei of cells were counterstained with 50 μg/mL propidium iodide (PI) (Beyotime Biotech Co., Ltd., China) at RT for another 5 min, and the fluorescence were observed with a confocal fluorescence microscope (Nikon C1-i, Japan).

Immunohistochemical staining

Four-week-old female nu/nu (Balb/C) mice were used to establish SiHa, HeLa, and A375 xenograft tumor models. Mice used in this study were purchased from the Shanghai Slac Laboratory Animal Co., Ltd. (Shanghai, China), and all animal experiment studies and protocols were approved by the Ethical Committee of Wenzhou Medical University. About 1×10^7cells/100 μL PBS were subcutaneously inoculated into the scapular region of nude mice. When the tumors size reached approximately 300–500 mm^3, the animals were sacrificed and the tumor samples were collected immediately and subsequently placed in 4% PFA overnight for immunohistochemical (IHC) staining or hematoxylin and eosin (HE) staining. After sectioning, the tissues were incubated with bispecific and monospecific affibody molecules (used as primary antibodies) for 1.5 h followed by incubation with mouse anti-His mAb overnight at 4 and HRP-conjugatedgoat-anti-mouse antibody at 37 °C for 1 h. Rabbit polyclonal anti-HPV16E7 and anti-HPV18E7 serum (prepared in-house) were used as positive control in IHC. In addition, the tissues were washed four times with PBS prior to incubation with either affibody or antibody.

Biodistribution of bispecific affibody molecules in tumor xenograft mice model

The dynamic distribution and tumor-targeting ability of the bispecific affibody were investigated in nude mice using near-infrared (NIR) optical imaging. Establishment of SiHa, HeLa, and A375 xenograft mice models have been described as above. Briefly, about 1×10^7cells/100 μL PBS were subcutaneously inoculated into the scapular region of nude mice. When the average tumor volume have reached approximately 300–500 mm^3, the xenograft mice model were used for NIR imaging. Dimeric and monomeric affibody molecules and

Z_{WT} affibody were labeled with Dylight-755 molecules (Thermo Fisher Scientific, USA) according to the manufacturer's recommendations. Subsequently, 100 μg of Dylight755-labeled affibody proteins dissolve in 200 μL PBS were injected via tail vein under isoflurane anesthesia, and the imaging was performed using an NIR Imaging System (CRi Maestro 2.10, USA) at various time points after injection. Additionally, the tumor/skin tissue ratio were analyzed at various time points post infection.

Results

Production of novel bispecific affibody molecule

The HPV16E7- and HPV18E7-targeting bispecific affibody molecule $Z_{HPV16E7}$–$Z_{HPV18E7}$ was subcloned for expression in *E. coli*. Additionally, two homodimeric $Z_{HPV16E7}$–$Z_{HPV16E7}$, $Z_{HPV18E7}$–$Z_{HPV18E7}$, and two corresponding monomeric control proteins $Z_{HPV16E7}$ and $Z_{HPV18E7}$ were expressed as His-tag fusion proteins in *E. coli*. In all dimeric constructs, the two E7 affibody molecules were joined by a peptide linker $(G_4S)_3$ (Fig. 1a). The linker peptide was flexible to facilitate separation of the two binding arms and maintain their particular three-dimensional (3D) structure (Lu and Feng 2008; Wen et al. 2013; Dall'Acqua et al. 1998). 3D structure prediction showed that the structure of each domain of dimers was similar to the natural structure of SPA-Z without conformational change (Fig. 1b). Thereafter, the His-tag fusion proteins were obtained by chromatography with Ni-NTA agarose and verified by SDS-PAGE and Western blot. The fusion proteins were successfully expressed with the size of about 15 kDa, which was consistent with the expected molecular weight. The results of Western blot showed that the fusion proteins could specifically react with mouse anti-His mAb (Fig. 1c). SDS-PAGE analysis showed that the purity of the final products was approximately 95%, which can be used for subsequent investigations.

Biosensor analysis

SPR biosensor assay was performed to verify the binding affinity of the bispecific affibody molecule to target proteins HPV16E7 and HPV18E7. The bispecific affibody molecule was injected at different concentrations over the flow-cell surfaces of a sensor chip containing immobilized recombinant HPV16E7 and HPV18E7, respectively. The results demonstrated a concentration-dependent increases in resonance

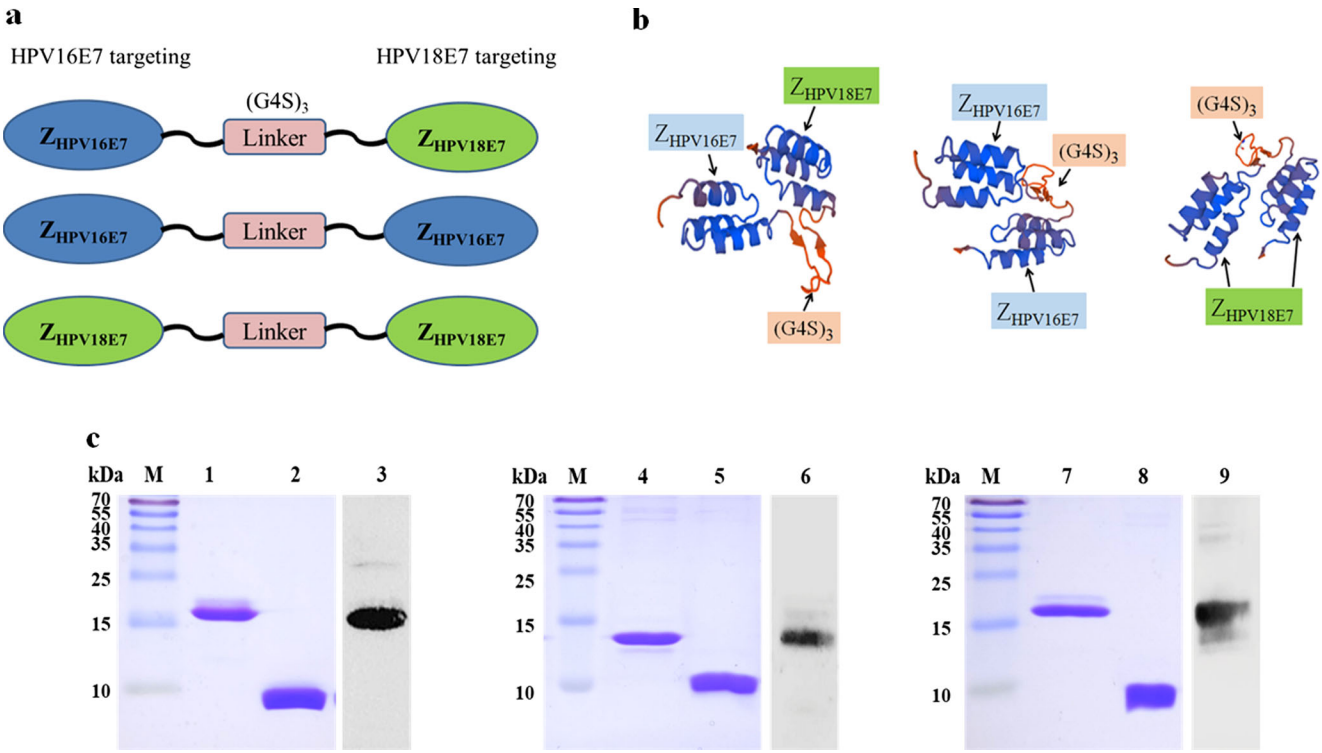

Fig. 1 Schematic presentation, SDS-PAGE, and Western blot analysis of the dimeric affibody molecules. **a** Schematic presentation of the dimeric affibody molecules. $Z_{HPV16E7}$, HPV16E7-specific affibody molecule; $Z_{HPV18E7}$, HPV18E7-specific affibody molecule; Linker, $(G_4S)_3$ peptide linker. **b** The predicted 3D structure of the dimeric affibody molecules. **c** SDS-PAGE and Western blot analysis of the purified affibody molecules. Lane 1, bispecific affibody molecule $Z_{HPV16E7}$–$Z_{HPV18E7}$; lane 2, Z_{WT}; lane 3, Western blot analysis of $Z_{HPV16E7}$–$Z_{HPV18E7}$; lane 4, $Z_{HPV16E7}$–$Z_{HPV16E7}$; lane 5, $Z_{HPV16E7}$; lane 6, Western blot analysis of $Z_{HPV16E7}$–$Z_{HPV16E7}$; lane 7, $Z_{HPV18E7}$–$Z_{HPV18E7}$; lane 8, $Z_{HPV18E7}$; lane 9, Western blot analysis of $Z_{HPV18E7}$–$Z_{HPV18E7}$; M, protein ladder. The mouse anti-His mAb served as the primary antibody in Western blot assay

signals and indicated the bispecific affibody molecule could bind directly to HPV16E7 and HPV18E7, respectively (Fig. 2). In terms of HPV16E7 ligand, the equilibrium dissociation constant (KD) of bispecific affibody molecule was 1.70×10^{-6} M, which was higher than that of monomeric $Z_{HPV16E7}$ (9.42×10^{-6} M) and homodimers $Z_{HPV16E7}$–$Z_{HPV16E7}$ (9.86×10^{-6} M) (Fig. 2a, c). Similar phenomenon was observed in HPV18E7 ligand, the KD of bispecific affibody molecules was 1.42×10^{-6} M, which was also higher than that of monomeric $Z_{HPV18E7}$ (5.96×10^{-6} M) and homodimers $Z_{HPV18E7}$–$Z_{HPV18E7}$ (1.22×10^{-5} M) (Fig. 2b, d). As expected, there was no interaction between the Z_{WT} and both surfaces (Fig. 2e, f). The results show clearly that the heterodimers ($Z_{HPV16E7}$–$Z_{HPV18E7}$) bind to the target oncoproteins HPV16E7 and HPV18E7 with high affinity.

Cell binding

The SPR biosensor assay revealed that the bispecific affibody molecule were able to bind to both recombinant HPV16E7 and HPV18E7. Thus, we investigated further whether the bispecific affibody molecule could also interact with the native HPV16E7 and HPV18E7 proteins within cancer cells by indirect immunofluorescence assay. As shown in Fig. 3, both SiHa cells (expressing HPV16E7 protein) and HeLa cells (expressing HPV18E7 protein) were recognized by the bispecific affibody molecule and brightly green fluorescence signals were observed in perinuclear area and nuclear membrane. As expected, there was no visible signals observed in cells incubated with Z_{WT} affibody molecule. Furthermore, only SiHa cells incubated with monomeric $Z_{HPV16E7}$ and

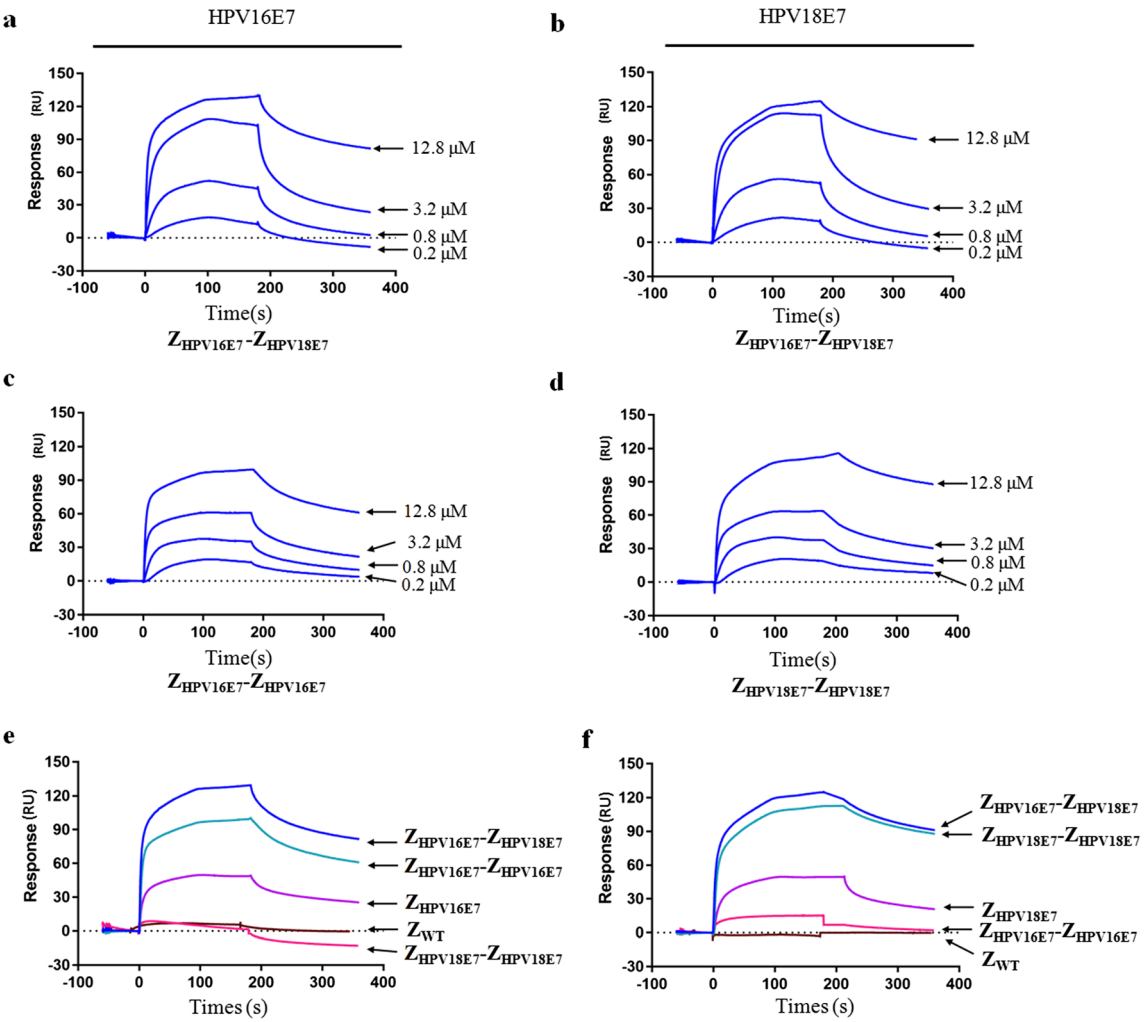

Fig. 2 SPR assay. Representative binding sensorgrams showing the interaction of bispecific affibody molecules with immobilized HPV16E7 (*left panel*) and HPV18E7 (*right panel*) proteins. **a**, **c** Sensorgrams obtained after injection of the $Z_{HPV16E7}$–$Z_{HPV18E7}$ or $Z_{HPV16E7}$–$Z_{HPV16E7}$ affibody molecules over a HPV16E7 flow-cell surface at selected concentrations—12.8, 3.2, 0.8, and 0.2 μM. **b**, **d** Sensorgrams obtained after injection of the $Z_{HPV16E7}$–$Z_{HPV18E7}$ or $Z_{HPV18E7}$–$Z_{HPV18E7}$ affibody molecules over a HPV18E7 flow-cell surface at selected concentrations—12.8, 3.2, 0.8, and 0.2 μM. **e**, **f** Sensorgrams obtained after injection 12.8 μM of the purified affibody molecules: $Z_{HPV16E7}$–$Z_{HPV18E7}$, $Z_{HPV16E7}$–$Z_{HPV16E7}$, $Z_{HPV18E7}$–$Z_{HPV18E7}$, $Z_{HPV16E7}$, and $Z_{HPV18E7}$ over a sensor chip flow-cell surface containing HPV16E7 or HPV18E7. Two independent experiments were performed and Z_{WT} was used as negative control

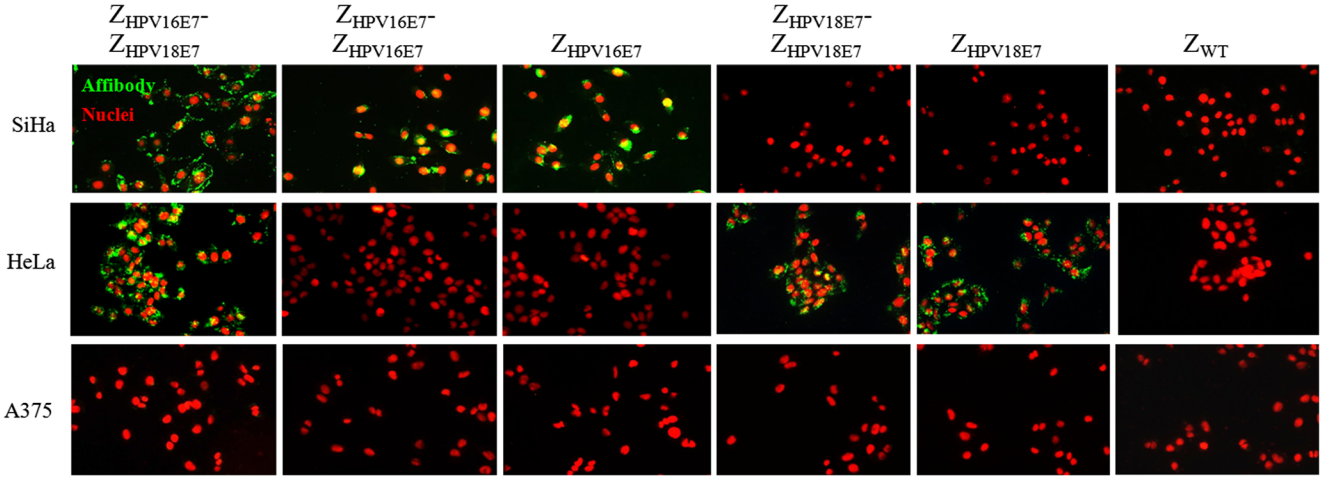

Fig. 3 Fluorescence staining of SiHa cells (expressing HPV16E7 protein) and HeLa cells (expressing HPV18E7 protein) with the heterodimers affibody molecules (× 400). FITC-conjugated goat anti-mouse IgG served as secondary antibody, and mouse anti-His-tag mAb which recognized His-tag of affibody was used to detect the affibody molecules (green). SiHa cells, HeLa cells, and HPV-negative A375 cell lines are labeled with the heterodimeric, homodimeric, and monomeric affibody molecules; Z_{WT} antibody molecule was set as control. The nuclei of cells were counterstained with PI (red)

homodimers $Z_{HPV16E7}$–$Z_{HPV16E7}$ showed brightly green fluorescence signals. Same phenomenon was observed in HeLa cells only labeled with monomeric $Z_{HPV18E7}$ and homodimers $Z_{HPV18E7}$–$Z_{HPV18E7}$. No fluorescence signal was observed in A375 cells when the cells were incubated with all the affibody molecules (Fig. 3). The data confirmed further that the bispecific affibody molecule could specifically bind to both HPV16E7 and HPV18E7 native proteins expressed within HPV positive carcinoma cell lines.

Immunohistochemistry (IHC)

To evaluate the simultaneous binding of the bispecific affibody molecule to HPV16E7 and HPV18E7 ex vivo, immunohistochemistry (IHC) was carried out on formalin-fixed paraffin-embedded xenograft tumor samples. Xenograft tumors were generated using SiHa, HeLa, and A375 cells. A standard IHC with anti-HPV16E7 polyclonal antiserum, anti-HPV18E7 polyclonal antiserum, and bispecific affibody molecule staining was performed on the xenografts collected when the average tumor size reached about 300–500 mm^3. IHC images of heterodimeric affibody molecule stained sections from SiHa xenograft showed brown signal, and similar patterns have been observed for anti-HPV16E7 polyclonal antibody, homodimeric $Z_{HPV16E7–HPV16E7}$ and monomeric $Z_{HPV16E7}$ labeling. However, there was no visible signal observed in sections incubated with homodimeric $Z_{HPV18E7–HPV18E7}$, monomeric $Z_{HPV18E7}$, Z_{WT} affibody molecules and PBS (Fig. 4). Similarly, images of heterodimeric affibody-stained sections from HeLa xenografts also showed brown signal, which displayed a similar pattern of anti-HPV18E7 polyclonal antibody labeling, homodimeric $Z_{HPV18E7–HPV18E7}$, and monomeric $Z_{HPV18E7}$. As expected, A375 xenografts did not show visible signal when the sections incubated with all the affibody molecules (heterodimers or homodimers) or polyclonal antibodies (against HPV16E7 or HPV18E7). Thus, IHC data demonstrated further that the bispecific affibody molecule could specifically bind to both HPV16E7 and HPV18E7.

Bispecific affibody molecule binds to targets and accumulated in tumor xenografts in vivo

To confirm further the biodistribution and in vivo tumor-targeting ability of heterodimeric affibody, nude mice bearing three cancer cell lines (SiHa, HeLa, and A375 cell lines) tumor xenografts were intravenously injected with Dylight755-labeled dimeric and monomeric affibody molecules (100 μg in 200 μ LPBS per mouse) and then scanned using an NIR imaging system at various time points after injection. As shown in Fig. 5a, fluorescence signal of Dylight755-labeled heteromeric affibody in subcutaneous xenografts of SiHa cells (HPV16E7 protein positive) and HeLa cells (HPV18E7 protein positive) was detectable at 0.5 h post-injection (p.i.). According to the tumor/skin ratio at different time points, we obtained the optical image with high contrast at 4 h p.i., and the fluorescence signal at tumor positions were maintained in both SiHa- and HeLa-derived xenografts over 48 h p.i. (Fig. 5a, c, and d). Additionally, the fluorescence signal of the Dylight755-homodimeric $Z_{HPV16E7–HPV16E7}$ and monomeric $Z_{HPV16E7}$ affibody molecules only occurred in the xenografts position of SiHa cells (HPV16E7 protein positive), whereas no visible fluorescence signal was observed in the xenograft position of HeLa cells (HPV18 E7 protein positive) (Fig. 5a). Optical images with high contrast were obtained at 2 h p.i. in SiHa-derived xenograft, and the fluorescence signal

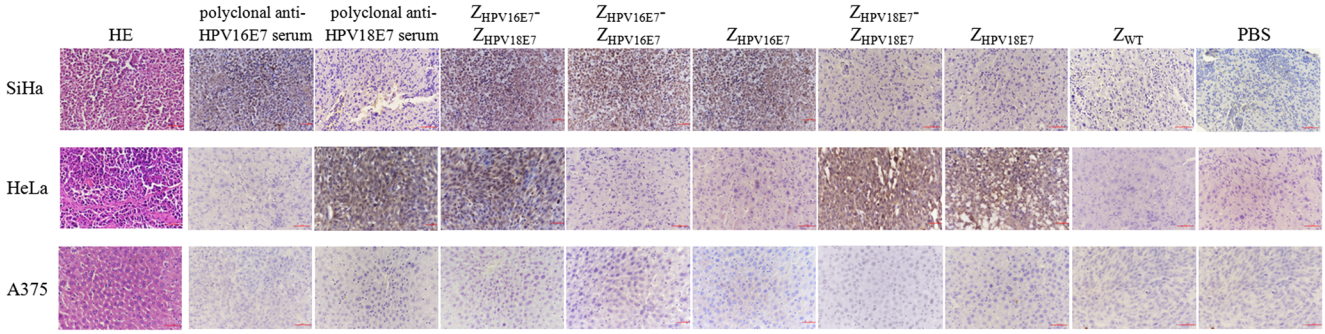

Fig. 4 Bispecific affibody molecule binds simultaneously to xenografts induced by either SiHa cells or HeLa cells. Representative image of SiHa-, HeLa-, or A375 cell-induced xenograft tissues by hematoxylin and eosin (HE) stain and immunohistochemistry (IHC) staining with bispecific affibody molecule. Sections from HPV16-positive SiHa xenografts (*upper panel*), HPV18-positive HeLa xenografts (*middle panel*), and HPV-negative A375 xenografts (*lower panel*) were respectively labeled with heterodimeric, homodimeric, and monomeric affiboby molecules, HPV16E7 and HPV18E7 polyclonal antiserum. Z_{WT} and PBS were set as negative control

at tumor positions were maintained over 24 h p.i. (Fig. 5a, c, and f). Similarly, the fluorescence signal of Dylight755-homodimeric $Z_{HPV18E7–HPV18E7}$ and monomeric $Z_{HPV18E7}$ affibody molecules only occurred in the tumor position of HeLa cells (HPV18E7 protein positive), whereas no visible fluorescence signal were observed in the xenograft position of SiHa cells (HPV16 protein positive) (Fig. 5a). Optical images with high contrast were obtained at 2 h p.i. in HeLa-derived xenograft, and the fluorescence signal at tumor positions were maintained over 12 h p.i. (Fig. 5a, d, and g).

In addition, accumulation in the kidneys was observed because the small size affinity proteins cleared via renal filtration. As expected, similar tumor-specific fluorescence signal were not detected in the xenografts position (both SiHa and HeLa cells) in mice injected with Dylight755-labeled Z_{WT} affibody (Fig. 5a). Meanwhile, no visible fluorescence signal was observed in the xenograft sites of A375 cell lines (HPV DNA negative) (Fig. 5b, e). These results demonstrated that the heterodimeric $Z_{HPV16E7–HPV18E7}$ affibody molecule could accumulate in the HPV16- and HPV18-derived tumor with high specificity in vivo.

Discussion

Unlike biopsy, molecular imaging in vivo can provide critical additional information including a global view of potential metastatic lesions in cancer diagnosis, therefore, molecular imaging has the great potential to improve the diagnosis of many diseases and to indicate appropriate treatment choices (Ståhl et al. 2017). Radionuclide molecular imaging of therapeutic targets is non-invasive and can be easily repeated to evaluate disease progression and monitor treatment effects (Tolmachev et al. 2010). The use of radiolabelled mAbs or bispecific antibodies is a more straightforward way to create molecular imaging agents. More recently, bispecific antibody blinatumomab (anti-CD3 and anti-CD19) has been approved for tumor therapy (Wu et al. 2015), therefore, development of bispecific antibodies as therapeutic or diagnostic agent has attracted strong attention (Yu et al. 2017; Schoffelen et al. 2010; McBride et al. 2006). However, mAbs and bispecific antibodies have some inherent limitations, such as large size due to the multidomain structure which may cause a less efficient tissue penetration.

Affibody molecules are a promising alternative to antibodies for development of bispecific binders because they are small (58 amino acids, ~ 6 kDa), disulfide-independent affinity protein (Löfblom et al. 2011). The very small size endows them efficient tumor penetration and rapid clearance from healthy tissues, which facilitates high-contrast imaging only a few hours after injection. The very rapid pharmacokinetics in vivo of this affinity protein makes them compatible with both longer-lived nuclides, such as ^{99m}Tc ($t_{1/2}$ 6 h) and ^{111}In ($t_{1/2}$ 2.8 days), for SPECT imaging or short-lived nuclides, such as ^{18}F ($t_{1/2}$110 min) and ^{68}Ga ($t_{1/2}$68 min), suitable for PET imaging (Wållberg and Ståhl 2013). Affibody-based tracers have been developed for imaging of molecular targets, such as HER2 (Orlova et al. 2006; Sörensen et al. 2014; Choi et al. 2016), EGFR (Cheng et al. 2016; Garousi et al. 2016), and HER3 (Rosestedt et al. 2015). Moreover, several preclinical and clinical studies have successfully demonstrated the potential of affibody-based agents (Wållberg and Ståhl 2013; Sörensen et al. 2014; Sörensen et al. 2016; Sandström et al. 2016).

The small molecular weight, absence of cysteine, and rapid folding, render the alternative affinity protein an excellent candidate for engineering of bi- and multispecific molecules. The molecular sizes of bi- or multispecific constructs based on affibody will remain to be smaller than the conventional antibody. Published data have shown that one bispecific affibody molecule targeting HER3 and HER2, which included an albumin-binding domain to allow a prolonged circulation time in vivo not only have a smaller molecular weight than scFv antibody fragment but also bind simultaneously to the two

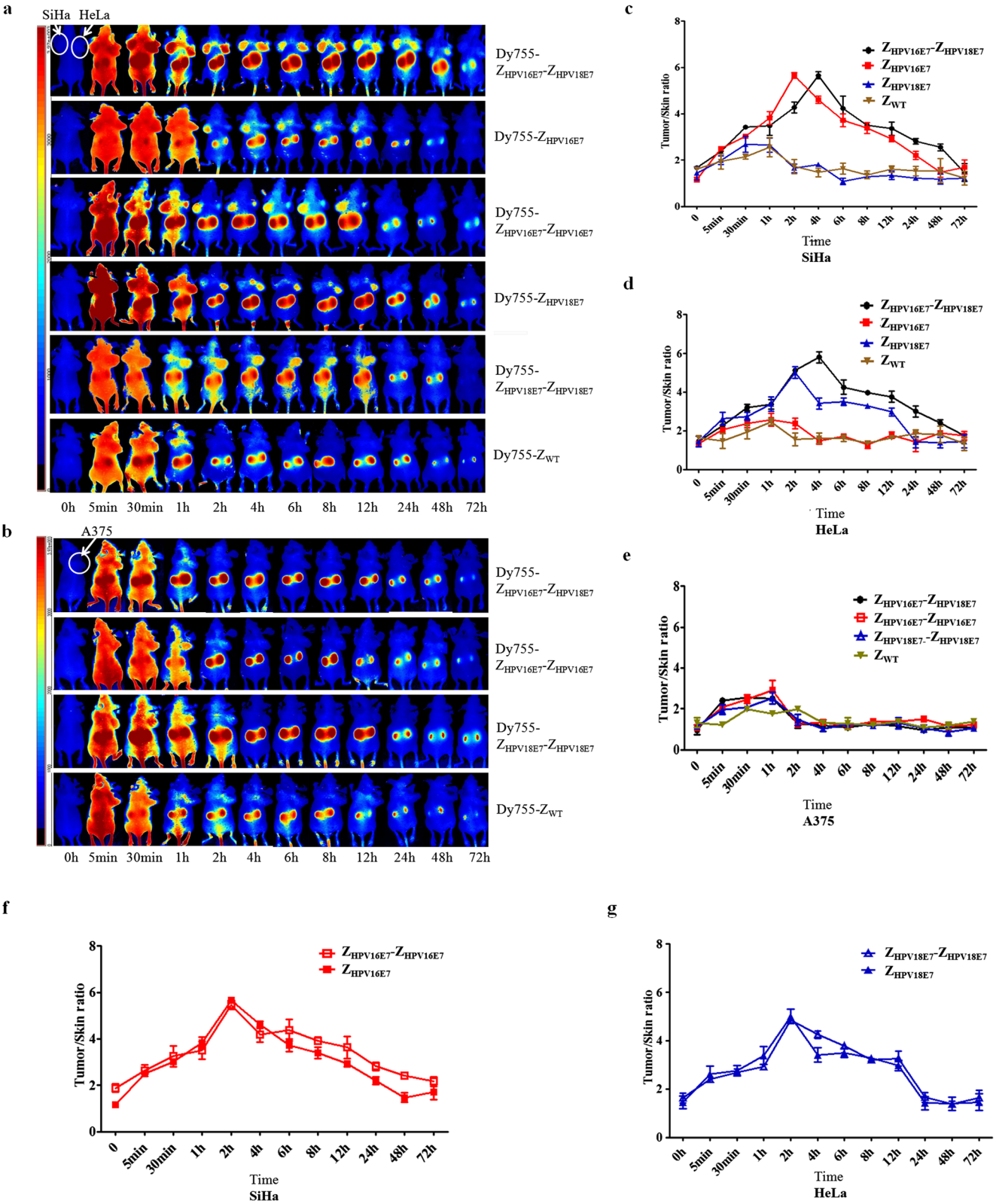

Fig. 5 Tumor uptake of heterodimeric affibody molecules. **a**, **b** In vivo uptake of affibody by subcutaneous tumor xenografts. Mice bearing SiHa, HeLa (**a**), and A375 cell (**b**) xenografts (circles) were intravenously injected with Dylight755-labeled heterodimer, homodimer, or monomer affibody molecules followed by dynamic scanning with in vivo NIR System. **c**–**g** Tumor-to-skin ratio of mice injected with Dylight755-labeled affibody molecules. All results were expressed as mean ± standard deviation (SD) ($n = 3$)

targets when investigated in biosensor assays (Malm et al. 2014). Similarly, another bispecific affibody targeting EGFR and HER2 was generated by genetic fusion of a Z_{EGFR} to a Z_{HER2} via a 20-amino-acid $(G_4S)_3$ linker. This bispecific affinity protein showed binding to both EGFR and HER2 in SPR biosensor and flow cytometry analysis (Ekerljung et al. 2012; Friedman et al. 2009). In our laboratory, we aim to develop bispecific affibody molecules targeting HPV16E7 and HPV18E7 oncoproteins that are derived from the two high-risk HPVs associated tightly with cervical cancer.

In our previous studies, we engineered affibody molecules respectively for specific binding of HPV16E7 (Xue et al. 2016) and HPV18E7 ($Z_{HPV18E7:228}$, Figs. S1 and S2) from phage display library. The affinity and specificity of the developed affibody molecules in binding to HPV16E7 and HPV18E7 have been confirmed by in vitro SPR biosensor assays and in vivo tumor xenografts. Here, we have generated a novel bispecific affibody molecule via $(G_4S)_3$ linker that binds simultaneously to two protein targets. 3D structure prediction showed that the structure of each domain of heterodimers and homodimers was similar to the natural format of SPA-Z without conformational change. Biosensor analysis demonstrated in vitro dual binding of the novel bispecific affinity molecule to HPV16E7 and HPV18E7 proteins. In addition, immunofluorescence analysis showed that the novel bispecific affibody molecule binds to HPV16E7 protein in SiHa cells and HPV18E7 protein in HeLa cells in in vitro cell cultures in a similar manner. IHC analysis confirmed that the novel bispecific affibody molecule binds simultaneously to the xenograft tumors in mice in vivo derived from either SiHa or HeLa cells. Thus, the novel bispecific affibody molecule $Z_{HPV16E7}$–$Z_{HPV18E7}$ can react with both HPV16 and HPV18 E7 oncoproteins against the tumors induced by the two high-risk HPV types in future diagnostic study.

Finally, the tumor uptake of heterodimeric affibody molecule was determined by an in vivo NIR system. Specific and quick accumulation of Dylight755-heterodimeric $Z_{HPV16E7}$–$Z_{HPV18E7}$ affibody were observed in SiHa and HeLa tumor xenografts in nude mice. Published study has shown that radiolabeled affibody $Z_{HER2:342}$ displayed a rapid tumor uptake in xenograft models and provided better contrast in HER2-positive SKOV-3 xenografts imaging than HER2-specific scFv antibody fragment (Orlova et al. 2006). Similar to the observation of previous studies (Orlova et al. 2006; Xue et al. 2016), we also observed that Dylight755-labeled bispecific affibody $Z_{HPV16E7}$–$Z_{HPV18E7}$ had deep penetration into tumors and quick clearance from the body when used for molecular imaging in vivo in subcutaneous xenografts mice model. Thus, bispecific affibody molecule generated in the present study used for tumor-specific fluorescence imaging may improve the accuracy of diagnosing and staging, indicating optimal treatment selection and thereby improve prognosis of cervical cancer.

In conclusion, we have used a $(G_4S)_3$ linker to develop a novel bispecific affibody molecule: $Z_{HPV16E7}$–$(G_4S)_3$–$Z_{HPV18E7}$, which targets both HPV16E7 and HPV18E7 oncoproteins. This bispecific affibody molecule has shown to detect simultaneously both HPV16-E7 and HPV18-E7 proteins in the two HPV-positive cancer cells through its binding to the two E7 oncoproteins in vitro and in vivo. Thus, the novel bispecific affibody molecule $Z_{HPV16E7}$–$(G_4S)_3$–$Z_{HPV18E7}$ developed in the present study has great potential for molecular imaging in cervical cancer caused by infection with HPV16 and HPV18 in the future.

Funding information This work was supported by the National Nature Science Foundation of China (81172463, 81502242) and the Public Welfare Foundation of Zhejiang Province (LGF18C010004).

Compliance with ethical standards

Conflict of interest The authors declare that they have no competing interest.

Ethical approval All applicable international, national, and/or institutional guidelines for the care and use of animals were followed. This study has been reviewed and approved by the ethics committee of the Wenzhou Medical University.

References

Andersson KG, Oroujeni M, Garousi J, Mitran B, Ståhl S, Orlova A, Löfblom J, Tolmachev V (2016) Feasibility of imaging of epidermal growth factor receptor expression with ZEGFR:2377 affibody molecule labeled with99mTc using a peptide-based cysteine-containing chelator. Int J Oncol 49(6):2285–2293. https://doi.org/10.3892/ijo.2016.3721

Badaracco G, Venuti A, Sedati A, Marcante ML (2002) HPV16 and HPV18 in genital tumors: significantly different levels of viral integration and correlation to tumor invasiveness. J Med Virol 67(4):574–582

Byrne H, Conroy PJ, Whisstock JC, O'Kennedy RJ (2013) A tale of two specificities: bispecific antibodies for therapeutic and diagnostic applications. Trends Biotechnol 31(11):621–632. https://doi.org/10.1016/j.tibtech.2013.08.007

Cheng Q, Wållberg H, Grafström J, Lu L, Thorell JO, Hägg O, Linder S, Johansson K, Tegnebratt T, Arnér ES, Stone-Elander S, Ahlzén HS, Ståhl S, Sel-tag imaging project (2016) Preclinical PET imaging of EGFR levels: pairing a targeting with a non-targeting Sel-tagged Affibody-based tracer to estimate the specific uptake. EJNMMI Res 6(1):58. https://doi.org/10.1186/s13550-016-0213-8

Choi JW, Hong ST, Kang DE, Paik KC, Han MS, Lim CS, Cho BR (2016) A two-photon tracer for human epidermal growth factor receptor-2: detection of breast cancer in a live tissue. Anal Chem 88(19):9412–9418

Dall'Acqua W, Simon AL, Mulkerrin MG, Carter P (1998) Contribution of domain interface residues to the stability of antibody CH3 domain homodimers. Biochemistry 37(26):9266–9273

de Sanjose S, Quint WG, Alemany L, Geraets DT, Klaustermeier JE, Lloveras B, Tous S, Felix A, Bravo LE, Shin HR, Vallejos CS, de Ruiz PA, Lima MA, Guimera N, Clavero O, Alejo M, Llombart-Bosch A, Cheng-Yang C, Tatti SA, Kasamatsu E, Iljazovic E, Odida M, Prado R, Seoud M, Grce M, Usubutun A, Jain A, Suarez GA, Lombardi LE, Banjo A, Menéndez C, Domingo EJ, Velasco J, Nessa A, Chichareon SC, Qiao YL, Lerma E, Garland SM, Sasagawa T, Ferrera A, Hammouda D, Mariani L, Pelayo A, Steiner I, Oliva E, Meijer CJ, Al-Jassar WF, Cruz E, Wright TC, Puras A, Llave CL, Tzardi M, Agorastos T, Garcia-Barriola V, Clavel C, Ordi J, Andújar M, Castellsagué X, Sánchez GI, Nowakowski AM, Bornstein J, Muñoz N, Bosch FX, Retrospective International Survey and HPV Time Trends Study Group (2010) Human papillomavirus genotype attribution in invasive cervical cancer: a retrospective cross-sectional worldwide study. Lancet Oncol 11(11):1048–1056. https://doi.org/10.1016/S1470-2045(10)70230-8

Ekerljung L, Wållberg H, Sohrabian A, Andersson K, Friedman M, Frejd FY, Ståhl S, Gedda L (2012) Generation and evaluation of bispecific affibody molecules for simultaneous targeting of EGFR and HER2. Bioconjug Chem 23(9):1802–1811

Fedorova A, Zobel K, Gill HS, Ogasawara A, Flores JE, Tinianow JN, Vanderbilt AN, Wu P, Meng YG, Williams SP, Wiesmann C, Murray J, Marik J, Deshayes K (2011) The development of peptide-based tools for the analysis of angiogenesis. Chem Biol 18(7):839–845. https://doi.org/10.1016/j.chembiol.2011.05.011

Frejd FY, Kim K (2017) Affibody molecules as engineered protein drugs. Exp Mol Med 49(3):e306. https://doi.org/10.1038/emm.2017.35

Friedman M, Lindström S, Ekerljung L, Andersson-Svahn H, Carlsson J, Brismar H, Gedda L, Frejd FY, Ståhl S (2009) Engineering and characterization of a bispecific HER2 x EGFR-binding affibody molecule. Biotechnol Appl Biochem 54(2):121–131. https://doi.org/10.1042/BA20090096

Garousi J, Andersson KG, Mitran B, Pichl M, Ståhl S, Orlova A, Löfblom J, Tolmachev V (2016) PET imaging of epidermal growth factor receptor expression in tumours using 89Zr-labelled ZEGFR:2377 affibody molecules. Int J Oncol 48(4):1325–1332. https://doi.org/10.3892/ijo.2016.3369

Hopman AH, Smedts F, Dignef W, Ummelen M, Sonke G, Mravunac M, Vooijs GP, Speel EJ, Ramaekers FC (2004) Transition of high-grade cervical intraepithelial neoplasia to micro-invasive carcinoma is characterized by integration of HPV 16/18 and numerical chromosome abnormalities. J Pathol 202(1):23–33

Kontermann RE (2012) Dual targeting strategies with bispecific antibodies. Mabs 4(2):182–197. https://doi.org/10.4161/mabs.4.2.19000

Kronqvist N, Malm M, Göstring L, Gunneriusson E, Nilsson M, Höidén Guthenberg I, Gedda L, Frejd FY, Ståhl S, Löfblom J (2011) Combining phage and staphylococcal surface display for generation of ErbB3-specific affibody molecules. Protein Eng Des Sel 24(4):385–396. https://doi.org/10.1093/protein/gzq118

Löfblom J, Feldwisch J, Tolmachev V, Carlsson J, Ståhl S, Frejd FY (2010) Affibody molecules: engineered proteins for therapeutic, diagnostic and biotechnological applications. FEBS Lett 584(12):2670–2680. https://doi.org/10.1016/j.febslet.2010.04.014

Löfblom J, Frejd FY, Ståhl S (2011) Non-immunoglobulin based protein scaffolds. Curr Opin Biotechnol 22(6):843–848. https://doi.org/10.1016/j.copbio.2011.06.002

Lu P, Feng MG (2008) Bifunctional enhancement of a β-glucanase-xylanase fusion enzyme by optimization of peptide linkers. Appl Microbiol Biotechnol 79(4):579–587. https://doi.org/10.1007/s00253-008-1468-4

Malm M, Bass T, Gudmundsdotter L, Lord M, Frejd FY, Ståhl S, Löfblom J (2014) Engineering of a bispecific affibody molecule towards HER2 and HER3 by addition of an albumin-binding domain allows for affinity purification and in vivo half-life extension. Biotechnol J 9(9):1215–1222. https://doi.org/10.1002/biot.201400009

McBride WJ, Zanzonico P, Sharkey RM, Norén C, Karacay H, Rossi EA, Losman MJ, Brard PY, Chang CH, Larson SM, Goldenberg DM (2006) Bispecific antibody pretargeting PET (immunoPET) with an 124I-labeled hapten-peptide. J Nucl Med 47(10):1678–1688

Mirabello L, Yeager M, Yu K, Clifford GM, Xiao Y, Zhu B, Cullen M, Boland JF, Wentzensen N, Nelson CW, Raine-Bennett T, Chen Z, Bass S, Song L, Yang Q, Steinberg M, Burdett L, Dean M, Roberson D, Mitchell J, Lorey T, Franceschi S, Castle PE, Walker J, Zuna R, Kreimer AR, Beachler DC, Hildesheim A, Gonzalez P, Porras C, Burk RD, Schiffman M (2017) HPV16 E7 genetic conservation is critical to carcinogenesis. Cell 170(6):1164–1174.e6. https://doi.org/10.1016/j.cell.2017.08.001

Muñoz N, Bosch FX, de Sanjosé S, Herrero R, Castellsagué X, Shah KV, Snijders PJ, Meijer CJ, International Agency for Research on Cancer Multicenter Cervical Cancer Study Group (2003) Epidemiologic classification of human papillomavirus types associated with cervical cancer. N Engl J Med 348(6):518–527

Ogilvie GS, Krajden M, Van Niekerk D, Smith LW, Cook D, Ceballos K, Lee M, Gentile L, Gondara L, Elwood-Martin R, Peacock S, Stuart G, Franco EL, Coldman AJ (2017) HPV for cervical cancer screening (HPV FOCAL): complete round 1 results of a randomized trial comparing HPV-based primary screening to liquid-based cytology for cervical cancer. Int J Cancer 140(2):440–448. https://doi.org/10.1002/ijc.30454

Orlova A, Magnusson M, Eriksson TL, Nilsson M, Larsson B, Höidén-Guthenberg I, Widström C, Carlsson J, Tolmachev V, Ståhl S, Nilsson FY (2006) Tumor imaging using a picomolar affinity HER2 binding affibody molecule. Cancer Res 66(8):4339–4348

Roman A, Munger K (2013) The papillomavirus E7 proteins. Virology 445(1–2):138–168. https://doi.org/10.1016/j.virol.2013.04.013

Romanczuk H, Howley PM (1992) Disruption of either the E1 or the E2 regulatory gene of human papillomavirus type 16 increases viral immortalization capacity. Proc Natl Acad Sci U S A 89(7):3159–3163

Ronco G, Dillner J, Elfström KM, Tunesi S, Snijders PJ, Arbyn M, Kitchener H, Segnan N, Gilham C, Giorgi-Rossi P, Berkhof J, Peto J, Meijer CJ, International HPV Screening Working Group (2014) Efficacy of HPV-based screening for prevention of invasive cervical cancer: follow-up of four European randomised controlled trials. Lancet 383(9916):524–532. https://doi.org/10.1016/S0140-6736(13)62218-7

Rosestedt M, Andersson KG, Mitran B, Tolmachev V, Löfblom J, Orlova A, Ståhl S (2015) Affibody-mediated PET imaging of HER3 expression in malignant tumours. Sci Rep 5:15226. https://doi.org/10.1038/srep15226

Sandström M, Lindskog K, Velikyan I, Wennbor A, Feldwisch J, Sandberg D, Tolmachev V, Orlova A, Sörensen J, Carlsson J, Lindman H, Lubberink M (2016) Biodistribution and radiation dosimetry of the anti-HER2 Affibody molecule 68Ga-ABY-025 in breast cancer patients. J Nucl Med 57(6):867–871. https://doi.org/10.2967/jnumed.115.169342

Saslow D, Solomon D, Lawson HW, Killackey M, Kulasingam SL, Cain J, Garcia FA, Moriarty AT, Waxman AG, Wilbur DC, Wentzensen N, Downs LS Jr, Spitzer M, Moscicki AB, Franco EL, Stoler MH, Schiffman M, Castle PE, Myers ER, ACS-ASCCP-ASCP Cervical Cancer Guideline Committee, American Cancer Society, American Society for Colposcopy and Cervical Pathology, American Society for Clinical Pathology (2012) American Society for Clinical Pathology screening guidelines for the prevention and early detection of cervical cancer. CA Cancer J Clin 62(3):147–172. https://doi.org/10.3322/caac.21139

Scheffner M, Werness BA, Huibregtse JM, Levine AJ, Howley PM (1990) The E6 oncoprotein encoded by human papillomavirus types 16 and 18 promotes the degradation of p53. Cell 63(6):1129–1136

Schoffelen R, Sharkey RM, Goldenberg DM, Franssen G, Mcbride WJ, Rossi EAChang CH, Laverman P, Disselhorst JA, Eek A, van der Graaf WT, Oyen WJ, Boerman OC (2010) Pretargeted immunopositron emission tomography imaging of carcinoembryonic antigen-expressing tumors with a bispecific antibody and a 68Ga- and 18F-labeled hapten peptide in mice with human tumor xenografts. Mol Cancer Ther 9(4):1019–1027. https://doi.org/10.1158/1535-7163.MCT-09-0862

Schwarz E, Freese UK, Gissmann L, Mayer W, Roggenbuck B, Stremlau A, zur Hausen H (1985) Structure and transcription of human papillomavirus sequences in cervical carcinoma cells. Nature 314(6006):111–114

Sörensen J, Sandberg D, SandströM M, Wennborg A, Feldwisch J, Tolmachev V, Åström G, Lubberink M, Garske-Román U, Carlsson J, Lindman H (2014) First-in- human molecular imaging of HER2 expression in breast cancer metastases using the 111In-ABY-025 affibody molecule. J Nucl Med 55(5):730–735. https://doi.org/10.2967/jnumed.113.131243

Sörensen J, Velikyan I, Sandberg D, Wennborg A, Feldwisch J, Tolmachev V, Orlova A, Sandström M, Lubberink M, Olofsson H, Carlsson J, Lindman H (2016) Measuring HER2-receptor expression in metastatic breast cancer using [68Ga]ABY-025 Affibody PET/CT. Theranostics 6(2):262–271. https://doi.org/10.7150/thno.13502

Ståhl S, Gräslund T, Eriksson KA, Frejd FY, Nygren PÅ, Löfblom J (2017) Affibody molecules in biotechnological and medical applications. Trends Biotechnol 35(8):691–712. https://doi.org/10.1016/j.tibtech.2017.04.007

Tolmachev V, Stone-Elander S, Orlova A (2010) Radiolabelled receptor-tyrosine-kinase targeting drugs for patient stratification and monitoring of therapy response: prospects and pitfalls. Lancet Oncol 11(10):992–1000. https://doi.org/10.1016/S1470-2045(10)70088-7

Walboomers JM, Jacobs MV, Manos MM, Bosch FX, Kummer JA, Shah KV, Snijders PJ, Peto J, Meijer CJ, Muñoz N (1999) Human papillomavirus is a necessary cause of invasive cervical cancer worldwide. J Pathol 189(1):12–19

Wållberg H, Ståhl S (2013) Design and evaluation of radiolabeled tracers for tumor imaging. Biotechnol Appl Biochem 60(4):365–383. https://doi.org/10.1002/bab.1111

Wen D, Foley SF, Hronowski XL, Gu S, Meier W (2013) Discovery and investigation of O-xylosylation in engineered proteins containing a (GGGGS)n linker. Anal Chem 85(9):4805–4812. https://doi.org/10.1021/ac400596g

Wu J, Fu J, Zhang M, Liu D (2015) Blinatumomab: a bispecific T cell engager (BiTE) antibody against CD19/CD3 for refractory acute lymphoid leukemia. J Hematol Oncol 8:104. https://doi.org/10.1186/s13045-015-0195-4

Xue X, Wang B, Du W, Zhang C, Song Y, Cai Y, Cen D, Wang L, Xiong Y, Jiang P, Zhu S, Zhao KN, Zhang L (2016) Generation of affibody molecules specific for HPV16 E7 recognition. Oncotarget 7(45):73995–74005. https://doi.org/10.18632/oncotarget.

Yu S, Li A, Liu Q, Yuan X, Xu H, Jiao D, Pestell RG, Han X, Wu K (2017) Recent advances of bispecific antibodies in solid tumors. J Hematol Oncol 10(1):155. https://doi.org/10.1186/s13045-017-0522-z